arXiv:2311.12401v3 [cs.CV] 15 Jan 2024

CASR: Refining Action Segmentation via Marginalizing Frame-levle Causal Relationships

Keqing Du
Xi'an Jiaotong University
dukeqing@stu.xjtu.edu.cn

Xinyu Yang
Xi'an Jiaotong University
yxyphd@mail.xjtu.edu.cn

Hang Chen
Xi'an Jiaotong University
albert2123@stu.xjtu.edu.cn

Abstract

Integrating deep learning and causal discovery has increased the interpretability of Temporal Action Segmentation (TAS) tasks. However, frame-level causal relationships exist many complicated noises outside the segment-level, making it infeasible to directly express macro action semantics. To address this issue, we propose ***Causal Abstraction Segmentation Refiner (CASR)****, which can refine TAS results from various models by enhancing video causality in marginalizing frame-level casual relationships. Specifically, we define the equivalent frame-level casual model and segment-level causal model, so that the causal adjacency matrix constructed from marginalized frame-level causal relationships has the ability to represent the segmnet-level causal relationships. CASR works out by reducing the difference in the causal adjacency matrix between we constructed and pre-segmentation results of backbone models. In addition, we propose a novel evaluation metric Causal Edit Distance (CED) to evaluate the causal interpretability. Extensive experimental results on mainstream datasets indicate that CASR significantly surpasses existing various methods in action segmentation performance, as well as in causal explainability and generalization. Our code will be available soon.*

1. Introduction

Temporal action segmentation (TAS) aims to identify and segment actions, has attracted a lot of attention in the fields of human-computer interaction [21, 22, 36], surveillance [13] and security[8, 20]. At the same time, the fusion of explainable AI [2, 32] and deep causal discovery [5, 9] increasingly becoming the mainstream of model selection. We all know there exists obviously causality in the video content [33, 35], so we can identify the causal relationships between frames to improve the performance of downstream tasks, such as learning temporal causal relationships in video frames [37], generating causal video summaries [15].

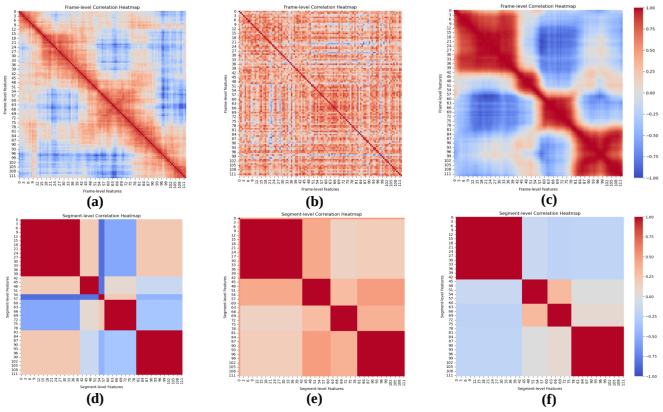

Figure 1. The feature similarity of the 5 action segments selected from the GTEA dataset[12], which is calculated by the cosine similarity of the features. The cooler the color, the lower the similarity; the warmer the color, the higher the similarity. (a)(b)(c) are the frame-level similarities respectively obtained from the original data, the segmentation results of MS-TCN++, and the segmentation results of MS-TCN++ with CASR. (d)(e)(f) are respectively the corresponding segment-level similarities of (a)(b)(c).

Although researchers have achieved improvements in the TAS task by capturing different temporal features and positioning boundary frames [11, 17, 27, 31], we find out that existing state-of-the-art models ignored the causal relationships contained in videos. In the meanwhile, we find this research gap can be attributed to the challenge of how to construct causal relationships between frames in long-form video, where frames are often used to be research units.

We exemplify the difficulty of constructing precise causal relationships between frames. As shown in Figure 1(a)(d), we calculate and visualize feature similarities in a piece of video data from frame-level (a) and segment-level (d) respectively. The relationship between frames is very complex, not only frames in one segment but also in different segments will exist correlation. This results in it being difficult to cluster macro segments directly according to frame-level causality. But in Figure 1(d), we find the adjacency matrix is

more regular from segment-level. The similarity between any two segments is far less than its self-loop similarity, and the segment-level matrix has the ability to reflect the action relationships in the frame-level matrix. We also calculated the feature similarity after segmentation through the mainstream TAS algorithm, as shown in Figure 1(b)(e). MS-TCN++ [19] is a good illustration of lacking causal explainability, the relationships at the frame-level became more confusing after action segmentation, and the similarity between segments increased instead.

In order to make causal relationships as evidence to improve the interpretability of action segmentation, we propose a ***C**ausal **A**bstraction **S**egmentation **R**efiner (CASR)*, which marginalizing some frame-level causal relationships to refine the segmentation results of backbone models. Here, the backbone models refer to any existing approaches for TAS task, such as classic and sota method MS-TCN [11]/ MS-TCN++ [19], ASRF [17], C2F-TCN [27] and CETNet [31]. Specifically, inspired by causal abstraction [3, 14], we define equivalent frame-level and segment-level causal models, so we can construct marginalized frame-level causal adjacency matrix according to segment-level causal adjacency matrix. Then, according to the pre-segment results from the backbone model, CASR constructs frame-level causal adjacency matrix through a self-supervised perspective. By learning the conditional probabilities between different frames, each frame can determine whether it belongs to the pre-segmentation. Our visualization results as shown in Figure 1(c)(f), the similarity between segments is reduced and they are obviously easier to segment. In addition, we propose a novel evaluation metric to measure the causal interpretability of segment results.

Our contribution can be summarized as follows:

- We propose Causal Abstraction Segmentation Refiner (CASR), which can refine the action segmentation results from the backbone model by marginalizing causal relationships in frame-level to enhance the causal interpretability of results. CASR can be plugged into various backbone models.
- Our approach can boost the performance of various SOTA action segmentation models, the novel evaluation metric *Causal Edit Distance* (CED) also confirmed. For example, on the 50Salads dataset, our model increases the segment edit distance of MS-TCN++ by 2.2% and that of C2F-TCN by 0.9%. On the Breakfast dataset, our model enhances the segment edit distance of ASRF by 4.6% and CETNet by 1.4%.

2. Preliminaries and Related Works

2.1. SCM & Causal Abstraction.

Structural Causal Model (SCM) is a conceptual model that describes the causal mechanism of a system, causal abstraction provides the equivalence conditions of SCMs at different levels in the same system. Based on these conceps, we will explain the causal mechanism in CASR in Section 3.

Definition 1 (Structural Causal Model (SCM) [24]) *A Structural Causal Model (SCM) is a 4-tuple* $\langle \mathbf{V}, \mathbf{U}, \mathcal{F}, \mathcal{P} \rangle$, *where* $\mathbf{V} = \{\boldsymbol{v}_i \mid i \in \mathbb{N}_n\}$ *are endogenous variables and* $\mathbf{U} = \{\boldsymbol{u}_i \mid i \in \mathbb{N}_m\}$ *are exogenous variables. Structural equations* $\mathcal{F} = \{f_i \mid i \in \mathbb{N}_n\}$ *are functions that determine* $\mathbf{V}$ *with* $v_i = f_i(\boldsymbol{pa}_i, \boldsymbol{u}_i)$, *where* $\boldsymbol{pa}_i \subseteq \mathbf{V}$ *and* $\boldsymbol{u}_i \subseteq \mathbf{U}$. $P(\boldsymbol{u})$ *is a distribution over* $\boldsymbol{u}$.

If we exert an intervention $\mathbf{V}^* \leftarrow \mathbf{v}^*(\mathbf{V}^* \subseteq \mathbf{V})$ on SCM, we will obtain a new SCM with different $\mathcal{F}$. Likewise, causal abstraction can map a low-level combination (SCM_L, I_L) with SCM_L and its intervention I_L to a high-level combination (SCM_H, I_H) with SCM_H and its intervention I_H. Under function mapping τ and intervention mapping ω, there exists $\tau(i_L(SCM_L)) = \omega_\tau(i_L)(SCM_H)$.

Definition 2 (τ-abstraction [3]) *Let* I_L *to be a set of interventions* $\mathbf{U}_L \leftarrow \boldsymbol{u}_L$ *on the low-level* $SCM_L = \langle \mathbf{V}_L, \mathbf{U}_L, \mathcal{F}_L, \mathcal{P}_L \rangle$, *and* I_H *be interventions on high-level* $SCM_H = \langle \mathbf{V}_H, \mathbf{U}_H, \mathcal{F}_H, \mathcal{P}_H \rangle$. *Let* τ *be a partial function* $\tau : \mathcal{D}(\mathbf{V}_L) \to \mathcal{D}(\mathbf{V}_H)$, *and let* $\omega : I_L \to I_H$ *be* $\omega_\tau(\mathbf{V}_L{}^* \leftarrow \boldsymbol{v}_L{}^*)$, *where* $\mathbf{V}_L{}^* \subseteq \mathbf{V}_L$,$\mathbf{V}_H{}^* \subseteq \mathbf{V}_H$,$\boldsymbol{v}_L{}^* \in \mathcal{D}(\mathbf{V}_L{}^*)$. *If* τ *and* ω_τ *are surjective and satisfy* $\forall i_L \in I_L : \tau(i_L(SCM_L)) = \omega_\tau(i_L)(SCM_H)$, (SCM_H, I_H) *is a* τ-*abstraction of* (SCM_L, I_L).

2.2. Related Works.

Causal abstraction. Rubenstein et al. [26]proposed the concept of *exact transformation* for the first time, using it to determine when a probabilistic causal model can be transformed into another model of the same system in causal consistency. The core of *exact transformation* is the mapping τ between causal models on different levels and the surjective map ω of hard interventions. To solve the problem of ignoring non-essential differences, Beckers and Halpern [3] further extended this concept to τ-abstraction, which requires two causal abstractions with soft interventions τ to induce a specific function ω. On the extremely end, there has been plenty of work to make causal abstract available in many fields. On the basis of category theory, Rischel and Weichwald [25] defines abstract $\langle \alpha = R, a, \alpha_{X^*} \rangle$ with a node set R of micromodel, mapping a between micromodel and macromodel, and surjective mapping set α_{X^*}; Otsuka and Saigo [23] defines abstract α by searching graph homomorphism from $\mathcal{G}_{\mathcal{M}^m}$ to $\mathcal{G}_{\mathcal{M}^M}$.

In this paper, we will use causal abstraction to demonstrate the equivalence of the frame-level and segment-level causal models we defined. In the subsequent sections, our frame-level is equivalent to the low-level and micromodel, while the segment-level corresponds to the high-level and macromodel.

Temporal Action Segmentation. Recently, methods based on deep learning can be mainly subdivided into those based on TCN, Transformer, and some fusion improvement methods. Many studies have introduced plugin techniques to enhance TCN-based models: GatedR [29] employed a gated forward refinement network, and Singhania et al. [27] developed a C2F-TCN encoder-decoder model. Particularly, MS-TCN [11] and MS-TCN++ [19] proposed multi-stage TCN to refine predictions iteratively across multiple temporal scales. Meanwhile, many improvement methods were proposed. ASRF [17] adds a branch to predict segmentation point information based on MS-TCN, and SSTDA [7] integrates a self-supervised model with MS-TCN.

Comparatively, Transformer-based models have emerged as a viable alternative to TCN. ASFormer [34] uses the encoder to process the video sequence and generate predictions, while the decoder takes predictions from previous layers as input. UVAST [4] employs a similar encoder, but predicts action segments autoregressively, effectively reducing over-segmentation. In a recent development, CETNet [31] employs a cross-enhancement transformer to efficiently learn temporal structure representations with interactive self-attention mechanisms and global and local information.

In addition, some methods of combining different backbone models for refining have emerged in recent years. Huang et al. [16] proposed a graph-based temporal reasoning module to learn the relation of multiple action segments in various periods, and construct R-GCN and C-GCN to respectively refine the boundary detection and frame division of the backbone model. Wang et al. [30] utilized a dilated temporal graph reasoning module, and constructed multi-level dilated temporal graphs to refine the segmentation result of the backbone model. Ahn and Lee [1] extracted different representations of video at frame-level, segment-level and video-level, and refined the out-of-context prediction results of the backbone model.

As previously noted, these studies have not focused on capturing the causal relationships between video contents, including the state-of-the-art models. Moreover, our work proposes Causal Abstraction Segmentation Refiner (CASR) on different backbone models, aiming to improve understanding and segmentation performance by simplifying causal relationships between frames.

3. Causal Relationship between frame & segment

In this section, we explained how to marginalize the causal relationships in frame-level and why. First of all, we can define the frame-level causal model and segment-level causal model of video modal according to the general definition of Structural Equation Model (SEM) [26].

Definition 3 (Frame-level Causal Model) *Frame-level causal model is composed of triples $M_X = (\mathcal{S}_X, \mathcal{I}_X, \mathbb{P}_E)$, where $X = (X_i : i \in \Xi_x)$ is the variable set contained all of the frames, structural equation $\mathcal{S}_X$ is the set of $X_i = f_i(X, E_i)$, $\mathcal{I}_X$ is a partially ordered set of perfectly interventions, and $\mathbb{P}_E$ is the distribution of the exogenous variable E*[1].

Definition 4 (Segment-level Causal Model) *Segment-level causal model is composed of triples $M_Y = (\mathcal{S}_Y, \mathcal{I}_Y, \mathbb{P}_E)$, where $Y = (Y_j : j \in \Xi_y)$ is the variable set contained all of the segments, structural equation $\mathcal{S}_Y$ is the set of $Y_j = f_j(Y, E_j)$, $\mathcal{I}_Y$ is a partially ordered set of perfectly interventions, and $\mathbb{P}_E$ is the distribution of the exogenous variable E.*

In order to ensure the identifiability of frame-level and segment-level causal models, we propose hypothesis1 according to the character of the video modal. In this way, we can satisfy the DAG (Directed Acyclic Graph) structure without proposing other assumptions such as acyclic constraints.

Hypothesis 1 (Causality Identifiability) *In the frame-level causal model, the variables X in $X_i = f_i(X, E_i)$ only contains $(X^*, \leq_{X_i})$, represents there is only the former variables (frames) have causal effect to the latter variables (frames) in the causal graph; likewise, the segment-level variables Y in $Y_j = f_j(Y, E_j)$ only contains $(Y^*, \leq_{Y_j})$, represents there is only the former segment have causal effect to the latter segment in the causal graph.*

In terms of hypothesis1, we can ensure the identifiability of the two causal models, this is consistent with the characteristic of causality from front to back in the video modality. Therefore, the two causal models can be transformed into each other. The proof process is presented in Appendix 7.

Definition 5 (Exchangeability) *When frame-level and segment-level causal model satisfy the Causality Identifiability 1, the two models can be transformed into each other.*

As previously mentioned, we have verified the frame-level causal model is susceptible to interference from noise terms. Although a complete action segment combines many frames, the complete and clear action semantic relationships in the video can only emerge at the segment-level. Therefore, when we only focus on action semantics, the noise relationship in the frame-level can be marginalized. This also explains why the frame-level and segment-level causal models can be transformed into each other. With regard to the Definition 5, we can process the frame-level causal relationships from the perspective of segment-level causal relationships.

[1]Exogenous variables are also referred to as noise variables in the literature. The same below.

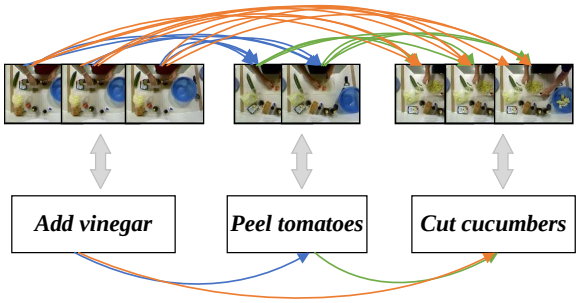

Figure 2. The causal relationships need to be considered in the frame-level causal model. Divide all the frames into several different parts according to their action segments in order, there only retains the causal relationship of one frame occurred first to the other frame occurred later, where two frames came from different action segments.

Corollary 1 (Frame-level Causal Relationships) *Assume that a complete video consists of M action segments $\{Y_1, Y_2, ..., Y_M\}$, where Y_i ($i \epsilon [1, M]$) represents different action segment. For any three variables $X_n^{Y_p}, X_l^{Y_p}, X_k^{Y_q}$ in the frame-level causal model M_X as an example, where $X_n^{Y_p}$ and $X_l^{Y_p}$ are respectively the n-th and l-th frames in the Y_p-th action segment, $n < l \leq T_{Y_p}$; $X_k^{Y_q}$ is the k-th frame in the Y_q-th action segment, $k \leq T_{Y_q}$. T_{Y_p} and T_{Y_q} represent the whole numbers of frames in action segments Y_p and Y_q, Y_p occurs before Y_q. Therefore,*

- *There is no causal relationship between two frames belonging to the same action segment in M_X, the conditional probability $P(X_l^{Y_p} | X_n^{Y_p}) \to 0$;*
- *There has a causal relationship between two frames belonging to the differnet action segment in M_X, when Y_p occurs first before Y_q, the conditional probability $P(X_k^{Y_q} | X_l^{Y_p}) \to 1, P(X_k^{Y_q} \mid X_n^{Y_p}) \to 1$*

In this way, only remains the relationships of frames came from different action segments. This visualization process as shown in Figure 2, takes three action segments as an example, which consist of 3, 2, and 3 frames respectively. The lines in blue represent the causal effect of "Add vinegar" to "Peel tomatoes", the lines in green represent the causal effect of "Peel tomatoes" to "Cut cucumbers", and the lines in orange represent the causal effect of "Add vinegar" to "Cut cucumbers". The marginalized causal relationships of frame-levle causal model are equivalent to the causal relationships of segment-levle causal model, our proposed CASR refines the segmentation of action segments by enhancing this frame-level causal relationship.

4. Methodology

4.1. Overall Structure

Figure 3 shows the overview of our CASR. CASR consists of two parts, Action Segment Engineer(ASE) and Causal Abstraction Refiner(CAR). It aims to refine the frame-level action segmentation result from a backbone model by strengthening the causal relationships between frames in different segments with self-supervision. According to the marginalized frame-level causal relationships, the core of CASR is to construct the causal adjacency matrix in ASE and CAR. Reducing the differences between the two through comparative learning, thereby refining the segmentation performance of action segment backbone models. We will elaborate on how ASE and CAR work out below.

4.2. Action Segment Engineer & Causal Abstract Refiner

After embedding original T frame images into features $X \in \mathbb{R}^{T \times n}$, where T is the sequence length, n is the feature dimension, X as an input of both ASE and CAR. The main component of ASE is action segment backbone models, including its networks and loss functions. Besides, we add a module to extract the pre-segmentation results and construct its causal adjacency matrix, which is used for contrastive learning to improve the causal adjacency matrix learned in CAR. We all know that any one action segment backbone model, will keep improving the segmentation result many times. The pre-segmentation results used here represent the first segmentation result predicted by the action segment backbone models. The first segmentation result focuses on short-term features between frame-level, so that the refined short-term features will affect the long-term features, thereby refining the segmentation performance of the entire model.

For pre-segmentation results $Y = \{y_1, y_2, \cdots y_K\}, y_i \in \mathbb{R}^{L \times M}$, where $M (M \in \mathbb{Z})$ is the number of action types, K is the number of action segments. We extract the action type $\hat{y}_i \in \mathbb{R}^L$ of i-th batch through the softmax function. Then, as mentioned in Corollary 1, we marginalized the frame-level causal relationships according to the equivalent segment-level causal relationships. Let the conditional probability $p(x_q^N | x_p^N)$ of any two frames in same action segment $N, (N \in [1, M])$ tends to 0, where $0 < p < q \leq T_N$. Likewise, the conditional probability $p(x_q^M | x_p^N)$ of any two frames in different action segment such as $N (N \in [1, M])$ and M should tends to 0, where $0 < p \leq T_N, 0 < q \leq T_M$, and segment N occurs before segment M. So the causal adjacency matrix of pre-segmentation result $C_i = [c_{pq}]$ is in terms of

$$c_{pq} = \begin{cases} 1, & \text{if } p \text{ and } q \text{ belong to different segments;} \\ 0, & \text{else} \end{cases} \quad (1)$$

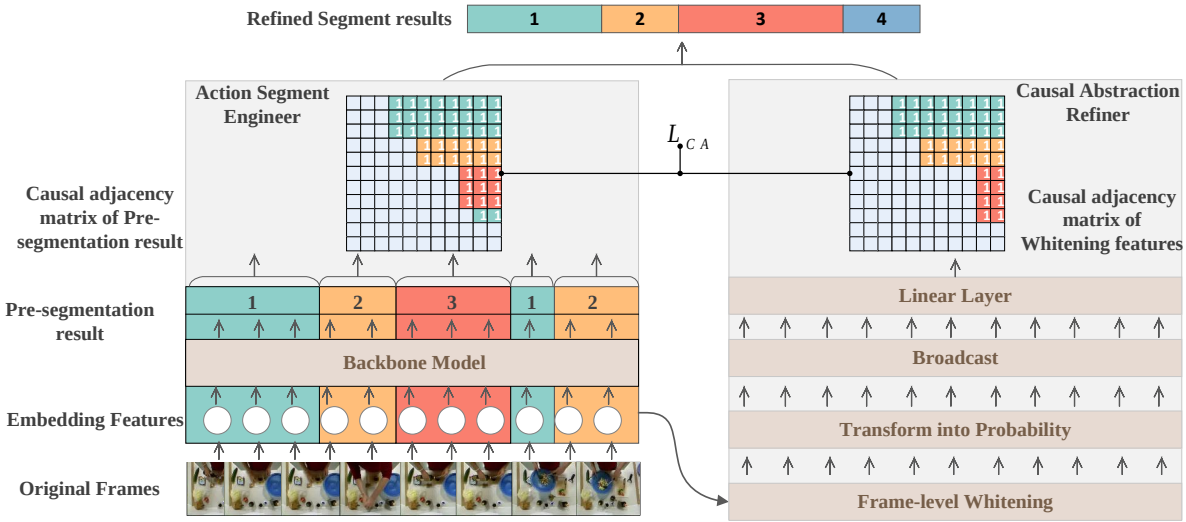

Figure 3. Overview of Causal Abstraction Segmentation Refiner (CASR). CASR aims to refine the action segmentation results that came from the backbone model in Action Segment Engineer (ASE). Causal Abstraction Refiner (CAR) extracts the embedding frame-level features, and learns the conditional probability between the frame-level whitening features. Based on marginalized frame-level causal relationships, constructing causal adjacency matrices of pre-segmentation result and whitening features separately, and reducing the difference between them.

CAR aims to learn the marginalized causal relationships in frame-levle causal model, making the causal adjacency matrix constructed by it as same as possible as the causal adjacency matrix constructed by the pre-segmentation results. In order to ensure the final learned results are frame-level relationships, CAR first whitens the embedding features to remove the correlation between frames. In order to improve calculation efficiency, we first divide the sequence into fixed-length K batches $\{x_1, x_2, \cdots, x_K\}$, $x_i \in \mathbb{R}^{L \times n}$, where L represents the batch size. By constraining $cov(x_i, x_i) = I$ among the features $\{x_1, x_2, \cdots, x_K\}$, perform singular value decomposition (SVD) on the feature matrix to obtain the whitened feature vector $Z = \{z_1, z_2, \cdots, z_K\}$. To ensure the stability of whitening, we follow the method in Ermolov et al. [10], randomly divide the sub-batch again, and then calculate the whitening matrix independently.

Regarding the whitened feature vector $\{z_1, z_2, \cdots, z_K\}$, the sigmoid function maps it to $[0, 1]$, represents the conditional probability between frame-level features.

$$p_i = sigmoid(z_i) \tag{2}$$

In the process of constructing the causal adjacency matrix, CAR utilized the broadcast mechanism to extend p_i to $P_i \in \mathbb{R}^{L \times L}$ in different dimensions.

$$P_i = p_i \oplus (L, 1) \tag{3}$$

$$P_i^T = p_i \oplus (1, L) \tag{4}$$

$\oplus$ is broadcast symbol. Similarly, we used a linear layer to learn the marginalized frame-level causal relationships of $P = \{P_1, P_2, \cdots, P_K\}$,

$$\hat{P}_i = W * P_i + b \tag{5}$$

where W and b are the weight and bias of the linear layer. $\hat{P}_i$ is the causal adjacency matrix of whitening features contains learned by CAR. CASR refined the final segment result by reducing the difference $\mathcal{L}_{CA}$ between $\hat{P}_i$ and the causal adjacency matrix C_i constructed from the pre-segmentation results.

4.3. Causality Representation Loss

Independent of the loss function of the backbone model in action segment engineer, we propose a new loss function $\mathcal{L}_{CA}$ for CASR to calculate the difference between $\hat{P}_i$ and C_i. The backbone model still contains its original loss function, such as the combined weighting of $\mathcal{L}_{TMSE}, \mathcal{L}_{CE}, \mathcal{L}_{TR}, \mathcal{L}_{AL}$. In CASR, $\mathcal{L}_{CA}$ is shrunken to frame-level to balance the relationship between $\mathcal{L}_{CA}$ and other backbone model loss functions.

$$\mathcal{L}_{CA} = \frac{1}{KL} \sum_{i=1}^{K} (C_i - \hat{P}_i)^2 \tag{6}$$

5. Experiment

In this section, we conduct sufficient experiments to answer the research questions:

- **RQ1:** How effective is CASR in refining the action segment backbone model on downstream tasks?
- **RQ2:** How about the generalization performance of CASR when applied to different action segment models?
- **RQ3:** Can CASR better learn the causal representation of data?

5.1. Settings

Datasets. In experiments, we use three challenging datasets: Georgia Tech Egocentric Activities (GTEA) [12], 50salads [28] and Breakfast [18]. The GTEA dataset consists of 28 first-person perspective videos containing 7 different daily activities performed by 4 actors, and the dataset is divided into 4 splits by actors. The 50salads dataset contains the entire process of 25 people making salads, with a total of 50 videos, and is divided into 5 splits. Breakfast dataset consists of 10 cooking activities performed by 52 different actors in multiple kitchen locations. This dataset is the largest of the three datasets and is divided into 4 groups. For consistency, all videos from these datasets are set to 15 fps. We use I3D [6] featureswhich are extracted from all frames and provided by Farha and Gall [11].

Evaluation Metrics. When evaluating action segmentation results, we use rolled-out frame-level segment labels from our CASR. For evaluation, frame-level accuracy (*Acc*), segmental edit distance (*Edit*), and segmental F1 scores with different overlapping threshold $k\%$ ($F1@k$) ($k = \{10, 25, 50\}$) are used. *Acc* is the most common value that reflects frame-level segmentation accuracy. Edit distance calculates the minimum number of operations required to perform a replacement operation between two frames, and measures the difference between two frames. Different overlap thresholds $k\%$ $F1$ can be used to evaluate the prediction quality of different time domain characteristics.

In order to evaluate the causal interpretability ability of segmentation results, we additionally propose Causal Edit Distance (*CED*) to measure the difference between causal adjacency matrix of the final segmentation results $\hat{C} \in \mathbb{R}^{T\times T}$ and ground truth $C \in \mathbb{R}^{T\times T}$. The construction method of the causal adjacency matrix is consistent with we proposed above in Section 4. Smaller *CED* values indicate a smaller discrepancy between the causal relationships among frame-level segmentation results and ground truth.

$$CED := avg(num(\hat{C}_{i,j} \neq C_{i,j})); i, j = 1, 2, \cdots, T \quad (7)$$

Baseline. We have selected several mainstream models and state-of-the-art models as baselines, and we have introduced it before, including TCN-based method MS-TCN++ [19] and C2F-TCN [27], Transformer-based method CETNet [31], and fusion-improved methods ASRF [17].

Implementation details. To mitigate random biases, our refiner applied to different baselines while preserving their original settings such as random seed, epochs, learning rate. All experiments are conducted on a single GEFORCE RTX 3090. To enhance training efficiency and prevent the occurrence of degenerate matrices during whitening, we configure the batch size for frames as 512. Furthermore, following the approach outlined in Ermolov et al. [10], we set the sub-batch size to 128.

5.2. Quantitative Results

In order to verify the effectiveness of our proposed CASR, we applied CASR to various state-of-the-art baseline models based on different backbones, such as MS-TCN++, ASRF, CETNet, and C2F-TCN. Table 1 shows the experiment results of our method, as well as the comparison with the baseline. Since our CASR needs to be trained by adding to different backbone models, in order to better test our refined segmentation performance, the baseline results we display are all our reproduction results under the same experimental conditions.

As shown in Table 1, the segmentation performance of CASR is significantly improved when applied to different backbone models (**RQ2**), especially in terms of the causal interpretability of the model (**RQ3**). Affected by the size of different datasets, *CED* measures the difference in the causal adjacency matrices of all frame-level models, so the range of its values is different under different data amounts. Under the same action segment backbone models and dataset, there is a significant improvement in causal interpretability with or without CASR. Every *CED* result with CASR applied is better than the original method. In cases where the amount of data is large (such as in the breakfast dataset), our segmentation performance improves significantly; in cases where the backbone model segmentation performance is relatively low (such as in MS-TCN++ and ASRF), our model performance gains also higher. (**RQ1**)

In the experiment, we whitened the frame-level feature vectors in order to remove the correlation between features and prevent all features from converging on a single point when learning conditional probabilities between frames. At the same time, we also normalized the loss learned by CASR to prevent the loss of $\mathcal{L}_{CA}$ from affecting the recognition of the model too much. We show different results without whitening and without normalizing the loss function in Table 2 respectively, which proves that whitening exactly has an important impact on learning the conditional probability between frame-levels, and normalizing $\mathcal{L}_{CA}$ helps to balance the relationship with the original loss function of the baseline model to improve segmentation performance.

[1] † represents the results is by our reproduction.

Table 1. Refinement results based on GTEA, 50salads,and Breakfast datasets.[1]

Methods	GTEA						50 Salads						Breakfast					
	$F1@10,25,50$			Edit	Acc	CED	$F1@10,25,50$			Edit	Acc	CED	$F1@10,25,50$			Edit	Acc	CED
MSTCN++†	82.3	83.6	71.9	79.8	77.6	8.400	79.4	77.3	69.3	71.6	82.8	3.334	62.8	56.7	44.6	64.3	66.3	78.223
MSTCN++† + CASR	86.4	84.2	72.7	80.8	78.9	7.942	81.6	79.7	71.4	73.8	84.0	2.869	66.3	60.5	48.0	70.6	70.6	48.691
Gain	4.1	0.6	0.6	1.0	1.3	-0.458	2.2	2.4	2.1	2.2	1.2	-0.465	3.5	3.8	3.4	6.3	4.3	-29.5
ASRF†	85.5	83.8	73.6	76.9	74.7	9.045	80.3	77.4	67.4	74.2	77.6	4.932	69.1	63.4	50.8	66.6	63.0	55.832
ASRF† + CASR	86.5	84.3	72.4	80.3	73.9	8.157	80.4	78.3	70.6	74.7	76.8	4.795	72.4	67.1	55.1	71.2	65.5	50.095
Gain	1.0	0.5	-0.8	3.4	-0.8	-0.888	0.1	0.9	3.2	0.5	-0.8	-0.137	3.3	3.7	4.3	4.6	2.5	-5.737
CETNet†	90.5	89.6	78.9	85.7	79.4	7.134	87.6	87.3	80.9	82.8	87.3	2.587	72.5	68.7	57.0	72.8	74.2	38.194
CETnet† + CASR	91.4	90.2	80.5	87.2	79.7	6.915	88.9	87.6	81.4	83.1	88.9	2.541	78.7	74.9	63.4	78.3	75.6	35.436
Gain	0.8	0.5	1.6	1.6	0.3	-0.219	1.3	0.3	0.5	0.3	1.6	-0.046	6.2	6.2	6.4	5.5	1.4	-2.8
C2F-TCN†	88	86.6	78.3	81.6	80.6	7.358	83.5	81.5	71.8	75.7	86.9	2.802	71.6	68.0	57.1	68.1	74.6	49.831
C2F-TCN† + CASR	88.7	87.7	78.8	83.5	80.7	7.023	83.9	81.6	72.9	76.6	86.7	2.603	71.9	68.2	57.2	67.6	75.7	48.327
Gain	0.7	1.1	0.5	1.9	0.1	-0.335	0.4	0.1	1.1	0.9	-0.2	-0.199	0.3	0.2	0.1	-0.5	1.1	-1.504

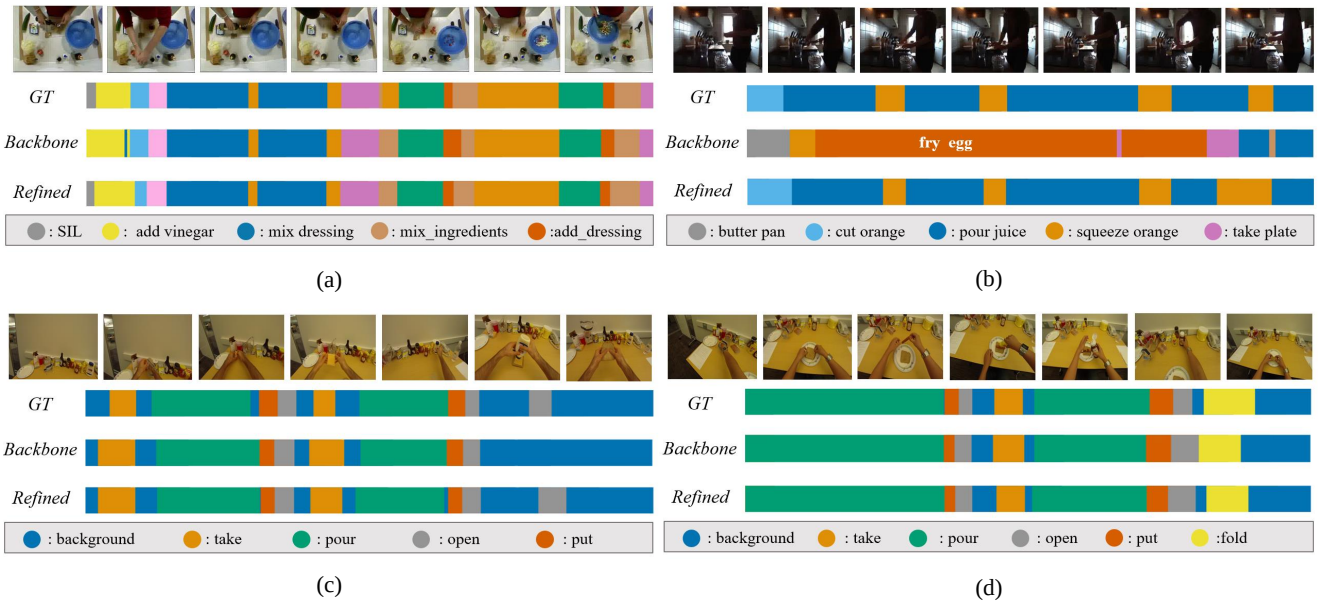

Figure 4. Qualitative results from HASR with various backbone models and datasets. Best view in color. (a) Refinement from MS-TCN++ with 50Salads dataset. (b) Refinement from ASRF with Breakfast dataset. (c) Refinement from CETNet with GTEA dataset. (d) Refinement from C2F-TCN with GTEA dataset.

Table 2. Ablation experiment result. Comparing contributions of normalization and whitening on the 50Salads dataset. Take MS-TCN++ as the backbone model as an example.

Model	$F1@10,25,50$			Edit	Acc	CED
w/ o normalization $\mathcal{L}_{CA}$ and whitening	77.9	75.5	67.2	69.9	81.9	3.298
w/ o whitening	78.9	76.2	68.1	71.4	82.2	3.255
w/ o normalization $\mathcal{L}_{CA}$	79.8	77.9	68.4	72.4	82.8	3.278
MSTCN++ + CASR (512,128)	**81.6**	**79.7**	**71.4**	**73.8**	**84.0**	**2.869**

Table 3. Comparing the effect of different batch sizes on the 50Salads dataset. Take MS-TCN++ as the backbone model as an example.

(Batch size, Sub-batch size)	$F1@10,25,50$			Edit	Acc	CED
(512,64)	75.4	72.5	61.9	70.5	79.3	3.719
(256,128)	76.6	74.2	65.2	69.0	81.1	3.502
(256,64)	75.3	73.4	64.2	68.4	78.8	3.982
(128,64)	77.1	74.6	65.2	69.9	80.8	3.453
Ours (512,128)	**81.6**	**79.7**	**71.4**	**73.8**	**84.0**	**2.869**

As previously mentioned, most of the action segment backbone models set batch size to 1, whose training unit is video. Owning to CASR aims to learn the frame-level causal relationships of one video so that the training unit here is frames in one video. We reset the batch size and sub-batch size from the frame-level to improve the efficiency of whitening and constructing the causal adjacency matrix.

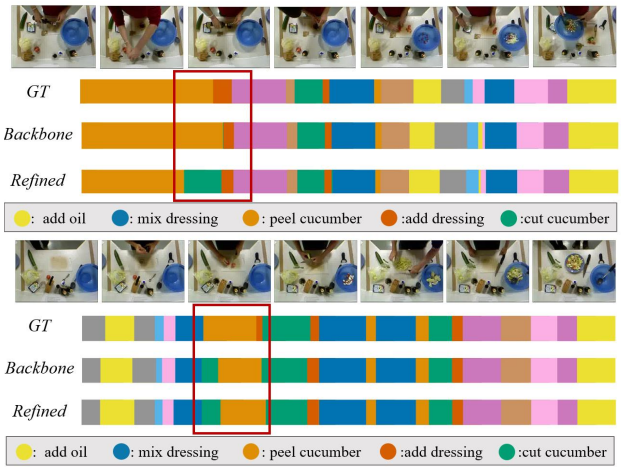

Figure 5. Some erroneous segmentation results caused by solidification of causal relationships. The results came from the 50Salads dataset, the backbone model is MS-TCN++. CASR obviously further amplifies this causal relationship (sucn as "Peel cucumber" $\rightarrow$ "Cut cucumber") solidified in backbone.

So we tested different batch sizes and sub-batch sizes respectively, and the results obtained are shown in Table 3. That is why we chose the combination *(512,128)* in our experiment. Selecting the batch size and sub-batch size as *(512, 128)* can effectively increase the training efficiency and maintain the stability of the gradient when facing thousands of total frames. When the difference between batch size and sub-batch size is 4 times, the heterogeneity of the whitening matrix can be better maintained and avoid matrix degradation.

5.3. Qualitative Results

As shown in Figure 4 (a), CASR can obviously correct over-segmentation errors. We have refined the phenomenon of the backbone model incorrectly identifying a small segment of other actions in one action segment, as well as incorrectly identifying the dividing points of adjacent action segments. Figure 4 (c) and (d) also show that CASR can identify some action segments not recognized by the backbone model, especially action segments with short duration, which refines the identification omission problem of the backbone model.

Figure 4 (b) shows the process of making orange juice from a third-person perspective. The backbone model obviously misidentified the main action segment as an action unrelated to the video content, such as "fry egg". This may also be due to the low brightness of the video. CASR can correct such out-of-context misrecognition, demonstrating CASR has excellent ability to identify and characterize the semantics of action segments.

5.4. Discussion.

During the experiment, we found that CASR may have a problem with the solidification of causal relationships. In the case where several action segments have nothing to do with each other, the segmentation results obtained may be unsatisfactory. As shown in Figure 5 (a)(b), in the ground truth *(GT)*, the action followed by "peel cucumber" is "add dressing" with low correlation, but because "peel cucumber" and "cut cucumber" have an extremely high correlation, so after the pre-segmentation result learns the "peel cucumber" action segment, some frames are divided into "cut cucumber".

Since CASR has a strong dependence on pre-segmentation results, our CASR amplifies this causal relationship based on the backbone, which instead leads to incorrect segmentation. Therefore, we hope to improve the solidified causal relationship in the next step of work. In this paper, we ignore the causal relationship between all frames within an action segment in order to enable the segment-level to represent action semantics more clearly, causing us to also ignore some fine-grained differences that may distinguish similar actions. Therefore, in the next work, we will consider the frame-level causality within the segment and design some new indicators to calculate the connection between frames. When this value exceeds a certain threshold, the two frames in one action segment are still considered to have a causal effect.

6. Conclusion

In this paper, we enhance the interpretability of temporal action segmentation tasks from a causality perspective. Our focus is on how to remove frame-level noise and simplify the frame-level causal model. To this end, we propose CASR to marginalize the noise relationship of frame-level causal models, which refines the performance of different backbone segmentation models. We also propose a novel evaluation metric CED to verify its causal interpretability. The core of CASR is to construct causal adjacency matrices for the frame-level causal relationships learned by ASE and CAR, and refine the segmentation performance of the backbone model in ASE by reducing the difference between two matrices. We have proven the effectiveness and generalization ability of CASR in a large number of experiments. In the future, we will build more interpretable models under various assumptions, improve the current possible problem of solidification of causal relationships, and reduce reliance on pre-segmentation results.

References

[1] Hyemin Ahn and Dongheui Lee. Refining action segmentation with hierarchical video representations. In *Proceedings of*

the IEEE/CVF International Conference on Computer Vision, pages 16302–16310, 2021. 3

[2] Plamen P Angelov, Eduardo A Soares, Richard Jiang, Nicholas I Arnold, and Peter M Atkinson. Explainable artificial intelligence: an analytical review. *Wiley Interdisciplinary Reviews: Data Mining and Knowledge Discovery*, 11 (5):e1424, 2021. 1

[3] Sander Beckers and Joseph Y Halpern. Abstracting causal models. In *Proceedings of the aaai conference on artificial intelligence*, pages 2678–2685, 2019. 2

[4] Nadine Behrmann, S Alireza Golestaneh, Zico Kolter, Juergen Gall, and Mehdi Noroozi. Unified fully and timestamp supervised temporal action segmentation via sequence to sequence translation. In *European Conference on Computer Vision*, pages 52–68. Springer, 2022. 3

[5] Jeroen Berrevoets, Krzysztof Kacprzyk, Zhaozhi Qian, and Mihaela van der Schaar. Causal deep learning. *arXiv preprint arXiv:2303.02186*, 2023. 1

[6] Joao Carreira and Andrew Zisserman. Quo vadis, action recognition? a new model and the kinetics dataset. In *proceedings of the IEEE Conference on Computer Vision and Pattern Recognition*, pages 6299–6308, 2017. 6

[7] Min-Hung Chen, Baopu Li, Yingze Bao, Ghassan AlRegib, and Zsolt Kira. Action segmentation with joint self-supervised temporal domain adaptation. In *Proceedings of the IEEE/CVF Conference on Computer Vision and Pattern Recognition*, pages 9454–9463, 2020. 3

[8] Giacomo De Rossi, Marco Minelli, Serena Roin, Fabio Falezza, Alessio Sozzi, Federica Ferraguti, Francesco Setti, Marcello Bonfè, Cristian Secchi, and Riccardo Muradore. A first evaluation of a multi-modal learning system to control surgical assistant robots via action segmentation. *IEEE Transactions on Medical Robotics and Bionics*, 3(3):714–724, 2021. 1

[9] Zizhen Deng, Xiaolong Zheng, Hu Tian, and Daniel Dajun Zeng. Deep causal learning: representation, discovery and inference. *arXiv preprint arXiv:2211.03374*, 2022. 1

[10] Aleksandr Ermolov, Aliaksandr Siarohin, Enver Sangineto, and Nicu Sebe. Whitening for self-supervised representation learning. In *International Conference on Machine Learning*, pages 3015–3024. PMLR, 2021. 5, 6

[11] Yazan Abu Farha and Jurgen Gall. Ms-tcn: Multi-stage temporal convolutional network for action segmentation. In *Proceedings of the IEEE/CVF conference on computer vision and pattern recognition*, pages 3575–3584, 2019. 1, 2, 3, 6

[12] Alireza Fathi, Xiaofeng Ren, and James M Rehg. Learning to recognize objects in egocentric activities. In *CVPR 2011*, pages 3281–3288. IEEE, 2011. 1, 6

[13] M Shamim Hossain, Ghulam Muhammad, and Atif Alamri. Smart healthcare monitoring: a voice pathology detection paradigm for smart cities. *Multimedia Systems*, 25:565–575, 2019. 1

[14] Yaojie Hu and Jin Tian. Neuron dependency graphs: A causal abstraction of neural networks. In *International Conference on Machine Learning*, pages 9020–9040. PMLR, 2022. 2

[15] Jia-Hong Huang, Chao-Han Huck Yang, Pin-Yu Chen, Andrew Brown, and Marcel Worring. Causal video summarizer for video exploration. In *2022 IEEE International Conference on Multimedia and Expo (ICME)*, pages 1–6. IEEE, 2022. 1

[16] Yifei Huang, Yusuke Sugano, and Yoichi Sato. Improving action segmentation via graph-based temporal reasoning. In *Proceedings of the IEEE/CVF conference on computer vision and pattern recognition*, pages 14024–14034, 2020. 3

[17] Yuchi Ishikawa, Seito Kasai, Yoshimitsu Aoki, and Hirokatsu Kataoka. Alleviating over-segmentation errors by detecting action boundaries. In *Proceedings of the IEEE/CVF winter conference on applications of computer vision*, pages 2322–2331, 2021. 1, 2, 3, 6

[18] Hilde Kuehne, Ali Arslan, and Thomas Serre. The language of actions: Recovering the syntax and semantics of goal-directed human activities. In *Proceedings of the IEEE conference on computer vision and pattern recognition*, pages 780–787, 2014. 6

[19] Shi-Jie Li, Yazan AbuFarha, Yun Liu, Ming-Ming Cheng, and Juergen Gall. Ms-tcn++: Multi-stage temporal convolutional network for action segmentation. *IEEE transactions on pattern analysis and machine intelligence*, 2020. 2, 3, 6

[20] Yong Liu, Weiwen Zhan, Yuan Li, Xingrui Li, Jingkai Guo, and Xiaoling Chen. Grid-related fine action segmentation based on an stcnn-mcm joint algorithm during smart grid training. *Energies*, 16(3):1455, 2023. 1

[21] Tianyu Luan, Yali Wang, Junhao Zhang, Zhe Wang, Zhipeng Zhou, and Yu Qiao. Pc-hmr: Pose calibration for 3d human mesh recovery from 2d images/videos. In *Proceedings of the AAAI Conference on Artificial Intelligence*, pages 2269–2276, 2021. 1

[22] Hao Ma, Zaiyue Yang, and Haoyang Liu. Fine-grained unsupervised temporal action segmentation and distributed representation for skeleton-based human motion analysis. *IEEE Transactions on Cybernetics*, 52(12):13411–13424, 2021. 1

[23] Jun Otsuka and Hayato Saigo. On the equivalence of causal models: A category-theoretic approach. In *Conference on Causal Learning and Reasoning*, pages 634–646. PMLR, 2022. 2

[24] Judea Pearl. *Causality*. Cambridge university press, 2009. 2

[25] Eigil F Rischel and Sebastian Weichwald. Compositional abstraction error and a category of causal models. In *Uncertainty in Artificial Intelligence*, pages 1013–1023. PMLR, 2021. 2

[26] Paul K Rubenstein, Sebastian Weichwald, Stephan Bongers, Joris M Mooij, Dominik Janzing, Moritz Grosse-Wentrup, and Bernhard Schölkopf. Causal consistency of structural equation models. *arXiv preprint arXiv:1707.00819*, 2017. 2, 3

[27] Dipika Singhania, Rahul Rahaman, and Angela Yao. Coarse to fine multi-resolution temporal convolutional network. *arXiv preprint arXiv:2105.10859*, 2021. 1, 2, 3, 6

[28] Sebastian Stein and Stephen J McKenna. Combining embedded accelerometers with computer vision for recognizing food preparation activities. In *Proceedings of the 2013 ACM international joint conference on Pervasive and ubiquitous computing*, pages 729–738, 2013. 6

[29] Dong Wang, Yuan Yuan, and Qi Wang. Gated forward refinement network for action segmentation. *Neurocomputing*, 407: 63–71, 2020. 3

[30] Dong Wang, Di Hu, Xingjian Li, and Dejing Dou. Temporal relational modeling with self-supervision for action segmentation. In *Proceedings of the AAAI Conference on Artificial Intelligence*, pages 2729–2737, 2021. 3

[31] Jiahui Wang, Zhengyou Wang, Shanna Zhuang, Yaqian Hao, and Hui Wang. Cross-enhancement transformer for action segmentation. *Multimedia Tools and Applications*, pages 1–14, 2023. 1, 2, 3, 6

[32] Feiyu Xu, Hans Uszkoreit, Yangzhou Du, Wei Fan, Dongyan Zhao, and Jun Zhu. Explainable ai: A brief survey on history, research areas, approaches and challenges. In *Natural Language Processing and Chinese Computing: 8th CCF International Conference, NLPCC 2019, Dunhuang, China, October 9–14, 2019, Proceedings, Part II 8*, pages 563–574. Springer, 2019. 1

[33] Xun Yang, Fuli Feng, Wei Ji, Meng Wang, and Tat-Seng Chua. Deconfounded video moment retrieval with causal intervention. In *Proceedings of the 44th International ACM SIGIR Conference on Research and Development in Information Retrieval*, pages 1–10, 2021. 1

[34] Fangqiu Yi, Hongyu Wen, and Tingting Jiang. Asformer: Transformer for action segmentation. *arXiv preprint arXiv:2110.08568*, 2021. 3

[35] Kexin Yi, Chuang Gan, Yunzhu Li, Pushmeet Kohli, Jiajun Wu, Antonio Torralba, and Joshua B Tenenbaum. Clevrer: Collision events for video representation and reasoning. *arXiv preprint arXiv:1910.01442*, 2019. 1

[36] Yuanhao Zhai, Ziyi Liu, Zhenyu Wu, Yi Wu, Chunluan Zhou, David Doermann, Junsong Yuan, and Gang Hua. Soar: Scene-debiasing open-set action recognition. In *Proceedings of the International Conference on Computer Vision*, 2023. 1

[37] Hongming Zhang, Yintong Huo, Xinran Zhao, Yangqiu Song, and Dan Roth. Learning contextual causality between daily events from time-consecutive images. In *Proceedings of the IEEE/CVF Conference on Computer Vision and Pattern Recognition*, pages 1752–1755, 2021. 1

CASR: Refining Action Segmentation via Marginalizing Frame-levle Causal Relationships

Supplementary Material

7. Proof of Exchangeability between causal models

We have proposed the frame-level causal model and segment-level causal model of video can be transformed into each other in Definition 5. We will prove the definition here.

Proof 1 *Let $\mathcal{M}_X = (\mathcal{S}_X, \mathcal{I}_X, \mathbb{P}_{E,F})$ be a liner frame-level causal model over the variables $W = (W_i : 1 \leq i \leq n)$ and $Z = (Z_i : 1 \leq i \leq m)$ with*

$$\begin{aligned} \mathcal{S}_X = \{W_i = E_i : 1 \leq i \leq n\} \cup \\ \{Z_i = \sum_{j=1}^{n} A_{ij} W_j + F_i : 1 \leq i \leq m\} \end{aligned} \tag{8}$$

$$\begin{aligned} \mathcal{I}_X = \{\varnothing, do(Z = z), do(W = w, Z = z) \\ : \omega \in \mathbb{R}^n, z \in \mathbb{R}^m\} \end{aligned} \tag{9}$$

and (E, F) $\mathbb{P}$ where $\mathbb{P}$ is any distribution over $\mathbb{R}^{n+m}$ and A is a matrix. Assume that there exists an $a \in \mathbb{R}$ such that each column of A sums to a. Consider the following transformation that averages the W and Z variables:

$$\tau : \mathcal{X} \to \mathcal{Y} = \mathbb{R}^2 \tag{10}$$

$$\begin{pmatrix} W \\ Z \end{pmatrix} \longmapsto \begin{pmatrix} \widehat{W} \\ \hat{Z} \end{pmatrix} = \begin{pmatrix} \frac{1}{n} \sum_{i=1}^{n} W_i \\ \frac{1}{m} \sum_{j=1}^{m} Z_j \end{pmatrix} \tag{11}$$

Futher, let $\mathcal{M}_Y = (\mathcal{S}_Y, \mathcal{I}_Y, \mathbb{P}_{\hat{E},\hat{F}})$ over the variables $\{\widehat{W}, \hat{Z}\}$ be a segment-level causal model of video with

$$\mathcal{S}_Y = \left\{\widehat{W} = \hat{E}, \hat{Z} = \frac{a}{m}\widehat{W} + \hat{F}\right\} \tag{12}$$

$$\begin{aligned} \mathcal{I}_X = \{\varnothing, do(\hat{W} = \hat{\omega}), do(\hat{Z} = \hat{z}), \\ do(hatW = \hat{\omega}, \hat{Z} = \hat{z}) : \hat{\omega} \in \mathbb{R}, \hat{z} \in \mathbb{R}\} \end{aligned} \tag{13}$$

$$\hat{E}\ \frac{1}{n} \sum_{i=1}^{n} E_i, \hat{F}\ \frac{1}{m} \sum_{i=1}^{m} F_i \tag{14}$$

Then segment-level $\mathcal{M}_Y$ is an exact τ-abstraction of frame-level $\mathcal{M}_X$.